Vadose Zone Journal
ORIGINAL RESEARCH

Numerical Simulation of Flow Dynamics during Macropore–Subsurface Drain Interactions Using HYDRUS

Onur Akay, Garey A. Fox,* and Jirka Šimůnek

Macropores, such as those created by deep-burrowing earthworms, have the potential to be hydraulically connected not only to the soil surface but also to subsurface drains. This hydraulic connection may lead to rapid movement of surface-applied chemicals to receiving waters as they bypass the bulk of the soil matrix. In this study, a numerical model (HYDRUS) that solves the three-dimensional Richards equation for both matrix and macropore domains was used to analyze previously conducted experiments that contained a single, surface-connected or buried, artificial macropore and a subsurface drain installed in a laboratory soil column. Both matrix and macropore domains were parameterized using continuous soil hydraulic functions. Simulations confirmed that surface-connected macropores were highly efficient preferential flow paths that substantially reduced arrival times to the subsurface drainage outlet, with this reduction being directly related to the length of the macropore. Surface-connected macropores need to extend at least halfway to the drain to have a noticeable effect (>50% reduction) on the arrival time. No significant changes were observed in total drain outflows for columns with laterally shifted macropores (away from a drain) compared with centered macropores unless the macropore depth extended significantly (>75%) into the profile. The model predicted that buried macropores became active and contributed to the total outflow only when pressure heads in the soil profile became positive. The effect of buried macropores on drain flow was investigated for a case where an initially partially saturated profile was drained. Under these conditions, the numerical simulations suggested that buried macropores could contribute up to 40% of the total outflow, which confirms laboratory observations with subsurface-drained soil columns with macropores.

ABBREVIATIONS: EF, express fraction; NS, Nash–Sutcliffe.

CONCERNS EXIST about the rapid transport of contaminants, such as pesticides (Fox et al., 2004), pathogens (Joy et al., 1998; Geohring et al., 1999; Jamieson et al., 2002; Shipitalo and Gibbs, 2005), and nutrients from the soil surface to groundwater through macropores (Magesan et al., 1995; Kladivko et al., 1999; Shipitalo and Gibbs, 2000). Commonly observed short-circuiting in many subsurface drainage field studies has been hypothesized to be due to direct hydrologic connectivity between macropores and subsurface drains (Fox et al., 2004, 2007; Shipitalo and Gibbs, 2000, 2005). Directly connected macropores can result in the rapid transport of contaminants from the soil surface into the subsurface drains and then into adjacent receiving streams and channels, bypassing the soil's filtering capacity. The ability to model the interrelationship between macropore-facilitated contaminant transport and subsurface drainage systems, where soil is consistently near saturation, is important for evaluating potential environmental contamination (Hoorman et al., 2005). In fact, Dorner et al. (2006) reported model simulations that predicted that most microorganisms entering streams enter from tile drainage rather than overland transport.

Column studies have been performed to answer questions regarding conditions when macropore flow occurs (Phillips et al., 1989; Trojan and Linden, 1992). Phillips et al. (1989) showed that water under negative pressures can enter simulated macropores after first establishing a continuous water film on the full length of the macropore walls. Trojan and Linden (1992) used 10 19-L, 29-cm-diameter buckets each packed with topsoil. After packing the buckets, 14 worms of species *Aporrectodea tuberculata* Eisen were placed on the soil surface. They concluded that the quantity of water that potentially can be delivered to a burrow is a function of initial soil water content, rainfall intensity and amount, hydraulic conductivity, and surface contributing area. Joschko et al. (1989) allowed earthworms (*Lumbricus terrestris* L.) to burrow into a soil column (19 cm wide and 40 cm long), artificially compacted to a pore volume of 40%. They demonstrated an exponential relationship between burrow depth and saturated hydraulic conductivity for the mainly vertically oriented *L. terrestris* burrows.

Several studies have included laboratory tests using undisturbed soil samples taken from macroporous fields (Shipitalo et al., 1990) or in situ tests using pan lysimeters or isolated blocks (Shipitalo and Edwards, 1996; Shipitalo et al., 1994). This approach permits an intact soil section to be analyzed under

O. Akay, Water Resources Group, PBS&J, Henderson, NV, formerly Dep. of Biosystems and Agricultural Engineering, Oklahoma State Univ.; G.A. Fox, Dep. of Biosystems and Agricultural Engineering, Oklahoma State Univ., 120 Agricultural Hall, Stillwater, OK 74078; J. Šimůnek, Dep. of Environmental Sciences, A135 Bourns Hall, Univ. of California, Riverside, CA 92521. Received 29 Aug. 2007. *Corresponding author (garey.fox@okstate.edu).

Vadose Zone J. 7:909–918
doi:10.2136/vzj2007.0148

controlled conditions, but it can become difficult to distinguish macropore effects from those introduced by the inherent complexity of natural soil systems.

In addition to the strategies discussed above to study macropore flow, there have been laboratory studies that utilized artificial macropores (Köhne and Mohanty, 2005; Ghodrati et al., 1999; Li and Ghodrati, 1997; Castiglione et al., 2003), which involves the creation of a macropore of known dimensions in a standardized soil. Although highly artificial, a standardized artificial soil eliminates the influence of textural and structural variations on the soil's physical behavior and permits study of the effect of individual macropore properties on soil physicochemical behavior (Buttle and Leigh, 1997). For example, Li and Ghodrati (1997) showed that at given normalized fluxes, preferential flow tends to occur to a greater extent in fine-textured soils than coarser textured soils, since coarser soils have much greater matrix conductivity than fine soils. Preferential flow also occurred under unsaturated water flow conditions. Laboratory studies with artificial macropores can also give an important insight into the effects of macropore tortuosity on breakthrough curves and solute distribution because of their well-defined macropore geometries (Allaire-Leung et al., 2000a,b).

The number of studies focused on the interaction between macropores and subsurface drains, however, are limited (Shipitalo and Gibbs, 2000; Shipitalo et al., 2004). Shipitalo and Gibbs (2000) observed macropores created by deep burrowing species of earthworms (*L. terrestris*) that allowed water to move directly to subsurface drains in a silt loam soil. Their research included the use of smoke injected into drain lines to observe its transmission to the soil surface. Smoke-emitting macropores were located within 50 cm of the drain line and the distance from the subsurface drains correlated with the infiltration rate. The rate at which water entered earthworm burrows declined with the logarithm of distance from the drain tile. Shipitalo and Gibbs (2005) investigated the importance of this connectivity by observing the structure of macropores and their surface connectivity (Fig. 1).

This "direct connectivity" phenomenon was verified by Akay and Fox (2007) by conducting infiltration experiments in a laboratory soil column with an artificial macropore placed directly above or shifted away from a subsurface drain. The experimental setup allowed the length of surface-connected or buried macropores to be varied without unpacking or disturbing the soil column between experiments. It was observed that the longer the buried macropore (i.e., as the macropore approached the soil surface), the more rapid the response at the drain outlet and the higher the fraction (35–40%) of the total drain flow that came from the macropore. Arrival times of drain flow for columns with surface-connected macropores (approximately eight times earlier than for columns with only matrix flow) decreased significantly compared with columns with buried macropores (only about two times earlier than for columns with only matrix flow). For experiments with 55-cm-deep surface-connected macropores, the average ratio of steady-state flow rates through macropores and matrix decreased as the lateral distance of the macropore from the drain increased: 2.4, 2.1, and 1.6 for distances of 0, 6.25, and 12.5 cm, respectively. An extrapolation of this trend suggests that only macropores located within 20 to 25 cm of the drain can be considered to be hydrologically directly connected.

FIG. 1. A photograph of a natural, directly connected macropore in the field preserved with polymer resin, demonstrating the connection between a macropore and a subsurface drain (courtesy of Martin Shipitalo, USDA-ARS, Coshocton, OH).

Steenhuis et al. (1997) modeled preferential transport to subsurface drains using a conceptual model based on two linear reservoirs located near the soil surface and closer to the drain. Their results suggested that methods based on field-averaged preferential flow characteristics are needed to model preferential flow to tile drains. Fox et al. (2004) modified a pesticide transport model, the Root Zone Water Quality Model (RZWQM), to include a direct connectivity using an express fraction (EF), which routes a user-specified fraction (estimated to be 2%) of water and contaminants through macropore flow directly from the soil surface to the drains. The estimated 2% EF was based on the assumption that directly connected macropores were located within 20 to 25 cm of the drain (a 10-m distance between subsurface drain lines) at the modeled field site in Allen County, Indiana, with silty clay soils. The modified model more appropriately captured the immediate breakthrough of pesticides during rainfall events shortly after pesticide application (Fox et al., 2004). Fox et al. (2007) evaluated the EF modification at an additional field site and suggested that EF must be calibrated to site-specific conditions, and ranged between 2 and 5% for the simulated field conditions. It is hypothesized that the larger site-specific EF could be a result of macropore–drain connectivity leading to shorter contact times for reactive solutes.

Because of the relatively limited modeling of macropore–subsurface drainage interactions using process-based models, we do not currently fully understand the water flow dynamics of drain systems influenced by surface-connected or buried macropores. Most laboratory column studies are limited to seepage face as opposed to subsurface drained bottom boundary conditions and most field studies are limited to measurements of breakthrough curves in tile drain flow. Therefore, the objective of this research was to improve our understanding of water flow dynamics in soils containing macropores in the vicinity of subsurface drains using a three-dimensional, finite-element, variably saturated flow numerical model. The modeling was verified using

the laboratory soil column experiments reported in Akay and Fox (2007). Specific questions to be addressed in this research included the following:

- Can a numerical model that uses different water retention and soil hydraulic functions to describe soil hydraulic properties of both macropore and matrix domains properly simulate flow in drained systems with either surface connected or buried macropores?
- Can the model confirm the commonly observed relationship between an increase in drain flow (and decrease in flow arrival time) with the macropore distance from the drain?
- Under what conditions do buried macropores become active contributors to subsurface drain flow?

Materials and Methods

Laboratory Column Studies

This research used data from the column studies of Akay and Fox (2007), which were constructed to simulate macropores in the vicinity of subsurface drainage. The 50-cm-wide by 28-cm-deep by 95-cm-long Plexiglas soil column consisted of a 6-cm perforated polyvinyl chloride subsurface drain tube installed in the center and approximately 2 cm above the impervious bottom of the soil column (Fig. 2). A sandy loam soil (55% sand, 32% silt, and 13% clay) was packed into the column to a height of 75 cm at a bulk density of 1.6 g cm^{-3}.

A 1-cm-diam. macropore was formed by wrapping a wooden rod with aluminum and nylon meshes. Macropores were either open at the soil surface (surface connected) and extending to different depths (15, 35, 55, and 75 cm) or fully buried, starting at a certain depth (3, 15, 35, and 55 cm) and ending at the depth of the drain. Macropores were located either at the center of the soil column above the drain or shifted 6.25 or 12.5 cm laterally. Matrix flow conditions were simulated with the wooden rod fully inserted through the column down to the drain. The wooden rod could be partially extracted to simulate various lengths of a buried macropore. For surface-connected macropores, the soil was packed to the lower part of the macropore and around the remaining length of the wooden rod, which was later fully extracted. Ponded water at the soil surface was allowed to enter surface-connected macropores but not buried macropores, which consisted of a soil buffer between the soil surface and the beginning of the macropore.

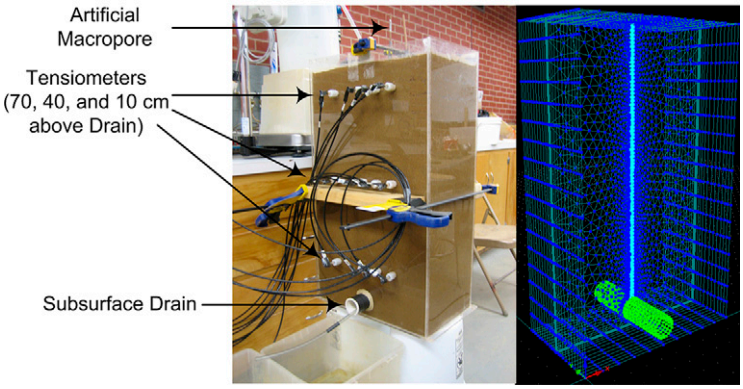

FIG. 2. The laboratory soil column and the corresponding three-dimensional computational domain in HYDRUS. The macropore is located at the center of the rectangular cross-section.

Soil pressure heads were monitored every 10 s at 10, 40, and 70 cm above the drain using four tensiometers (bubbling pressure = 100 cm H_2O, Soil Measurement Systems, Tucson, AZ) equipped with pressure transducers (ASDX001, Invensys, Milpitas, CA) spaced along a horizontal plane at 12.5, 25.0, 31.5, and 38.0 cm from the left side of the column. The tensiometer–transducer system had a range of 5 to −70 cm H_2O. A datalogger (CR10X, Campbell Scientific, Logan, UT) continuously received and transmitted information to a computer for automated pressure monitoring. Digital scales (EK-12Ki, A&D, Milpitas, CA) recorded the outflow from the subsurface drain for shifted and centered surface-connected macropore experiments. For centered, buried macropore experiments, a tube was run from the top of the drain where the macropore entered to a separate scale. The scales recorded outflow from both the macropore (discharge from the tube connected to the bottom of the macropore) and the soil matrix (collected from the subsurface drain tube) for centered buried macropore experiments (see Akay and Fox, 2007, Fig. 2).

For all experiments (i.e., centered and shifted, surface-connected and buried macropores), a Marriott-type infiltrometer created a 1-cm ponded water layer at the soil surface for either two or 3 h (referred to as the *infiltration* component of the experiments). Data collection of pressure heads and drain flow continued for 24 h after the water supply was turned off (referred to as the *drainage* component of the experiments).

Numerical Model Simulations

The experiments were simulated using the three-dimensional HYDRUS code. The HYDRUS program is a finite-element model for simulating two- and three-dimensional movement of water, heat, and multiple solutes in variably saturated media. The HYDRUS code numerically solves the Richards equation for saturated–unsaturated water flow (Šimůnek et al., 2006). Due to sharp interfaces between the macropore and matrix domains, a fine finite-element grid around the macropore (Δx_{min} = 0.15 cm), as well as small time steps (Δt_{min} = 10^{-10} h), were used to maintain numerical stability. In contrast to earlier studies in which dual-porosity and dual-permeability one-dimensional models with either first-order (Castiglione et al., 2003; Šimůnek et al., 2003) or second-order (Köhne and Mohanty, 2005) mass transfer terms were used, this study involved a single flow (Richards) equation used for the entire three-dimensional transport domain, including both the matrix and a macropore. Earlier work by Köhne and Mohanty (2005) demonstrated that, for a laboratory column packed with soils having two distinctive soil hydraulic functions, utilization of a pseudo-three-dimensional axisymmetrical Richards equation provided more accurate results than dual-permeability models with first- and second-order mass transfer terms. The van Genuchten–Mualem model (van Genuchten, 1980) was used to describe the water retention, $\theta(h)$, and conductivity, $K(h)$, functions for both matrix and macropore domains:

$$\theta(h) = \begin{cases} \theta_r + \dfrac{\theta_s - \theta_r}{\left[1 + |\alpha h|^n\right]^m} & h < 0 \\ \theta_s & h \geq 0 \end{cases} \quad [1]$$

$$K(h) = K_s S_e^l \left[1 - \left(1 - S_e^{1/m}\right)^m\right]^2$$
$$m = 1 - 1/n, \quad n > 1 \qquad [2]$$

where $S_e = (\theta - \theta_r)/(\theta_s - \theta_r)$ is the effective saturation; α [L^{-1}], n, and l are empirical parameters; θ_s is the saturated water content [L^3 L^{-3}]; θ_r is the residual water content [L^3 L^{-3}]; and K_s [$L\,T^{-1}$] is the saturated hydraulic conductivity. A three-dimensional numerical grid comprising 31 vertical layers was constructed (Fig. 2). The number of finite-element nodes ranged between 25,460 and 53,692, depending on the length of the simulated macropore.

The boundary conditions for the numerical model were chosen according to the experimental conditions used by Akay and Fox (2007). The constant pressure head (1-cm) boundary condition was used at the top of the soil profile during the first 2 or 3 h to simulate infiltration. The boundary condition was then switched to a no-flux boundary condition at the end of the infiltration period to simulate the redistribution and drainage parts of the laboratory experiment. The seepage face boundary condition was specified along a cylinder representing the 6-cm-diameter subsurface drain that was located 2 cm above the no-flux base boundary. A seepage face boundary acts as a zero pressure head boundary for nodes that are saturated and a no-flux boundary for nodes that are unsaturated. When simulating the laboratory experiments, the initial condition in the flow domain was specified based on tensiometer readings obtained from the laboratory study, with a pressure head of 2 cm at the bottom (i.e., maintaining a zero pressure head at the base of the subsurface drain) and –77 cm at the soil surface.

Observations were made regarding the conditions necessary for the development of flow in the buried macropore regime. Buried macropores become active only when positive pressures develop in their vicinity in the matrix domain. In simulating the infiltration experiments with buried macropores, the model was not able to predict macropore flow due to simulating the drain as a seepage face boundary condition (i.e., no pressure buildup was simulated in the matrix in the vicinity of the macropore). The subsurface drain represented as a seepage face boundary in the model was, in fact, a perforated tube with <10% open area. In addition, fine migrating particles may become lodged in these small openings, clogging the soil–drain interface and increasing the resistance to flow. Therefore, the laboratory drain did not act as a true seepage face boundary.

Since no detailed information was available on the degree of restriction at the drain, a hypothetical drainage scenario was simulated with buried macropores. Numerical simulations were performed for a scenario in which the water table was initially above the subsurface drain. Such cases can be observed in subsurface drain management applications. For example, controlled drainage systems are being applied to subsurface-drained fields to reduce NO_3 losses by placing a weir in the drainage outlet so as to raise the water level in the outlet and reduce subsurface drainage rates (Skaggs et al., 1995). This type of management practice can raise the average groundwater level to 20 to 25 cm below the ground level (Wesstrom and Messing, 2007; Skaggs et al., 1995). As a result of the high water table, the otherwise ineffective buried macropores can transmit significant flow due to their relatively high conductance during lowering of the groundwater level. Even though controlled drainage has been found to reduce NO_3–N and P losses by 35 to 45% (Skaggs et al., 1994), the response of the preferential flow paths is not yet understood.

For the hypothetical scenarios with buried macropores, the boundary condition at the bottom of the macropore was set to zero pressure head to simulate its direct connection to the subsurface drainage system (buried macropores are open to the atmosphere through the subsurface drain), whereas the seepage face boundary condition was used for the remainder of the drain in contact with the matrix domain. A no-flux boundary condition was used at the soil surface. Simulations included buried macropores with various lengths (i.e., 15, 35, 55, and 80 cm) and various initial water table levels (i.e., 15, 35, 55, and 80 cm above the top of the drain). The column dimensions remained the same as in simulations with surface-connected macropores.

The van Genuchten (1980) model parameters for the matrix domain were obtained using inverse estimation and the laboratory column infiltration experiment without a macropore, i.e., involving only matrix flow. Inverse estimation methods allow the most suitable model description of experimental data (Köhne and Mohanty, 2005). During inverse estimation, an objective function that represents deviations between measured and calculated space–time variables and soil hydraulic properties is minimized. Minimization of this objective function can be accomplished using the Levenberg–Marquardt nonlinear minimization method (Šimůnek et al., 2006). The space–time variable chosen for the parameterization of the matrix flow model (without a macropore) was the cumulative subsurface drain flow obtained from the laboratory experiment. The soil hydraulic parameters K_s, α, and n were optimized, whereas θ_s and θ_r were fixed and hence excluded from the inverse estimation process. Initial estimates of the soil hydraulic parameters for K_s, α, and n and the fixed values of θ_s and θ_r were obtained from the water retention analysis conducted on a soil core sample extracted from the laboratory column of Akay and Fox (2007). Water retention was determined on undisturbed soil cores using Tempe cells for 0- to 1000-cm pressures. For pressures >1000 cm, water retention was determined on disturbed soil samples by the pressure plate extractor method. The RETC code (van Genuchten et al., 1991) was used to fit the van Genuchten parameters of θ_s, α, and n (Table 1) based on data from this undisturbed soil core (Akay and Fox, 2007).

The K_s value of the macropore domain was the only van Genuchten (1980) parameter adjusted by a trial-and-error process to match the cumulative drain flow for the laboratory experiment with the 55-cm, centered, surface-connected macropore. The other parameters were held constant to reflect a small air-entry pressure (high α value), below which the hydraulic conductivity reduced to negligible values (high n value) (Castiglione et al., 2003). Using the calibrated value of the macropore-domain K_s, various simulations were performed with centered and shifted, surface-connected macropore lengths (i.e., 15, 25, 35, 45, 55, 65, and 70 cm) and the ratios of total to matrix steady-state discharge relative to macropore length were compared.

In contrast to surface-connected macropores, the van Genuchten (1980) parameters of θ_s, α, and n were found to significantly influence the exchange between the matrix and buried macropores. Two sets of fixed parameters (θ_s = 1.0, α = 1 cm^{-1}, n = 2 or 6) were used in the presented simulations. Two values of n (2 and 6) were used to show the sensitivity of the model

to this parameter, where n = 2 was selected to represent a value for a typical soil and n = 6 was selected to obtain an immediate release of water from saturated to residual moisture content. Theoretically, an infinite n would be required to represent the immediate decline in θ from θ_s to θ_r with increases in the soil pressure head. The percentage of drain flow entering the drain from the macropore and the matrix was calculated.

Results and Discussion

Calibration to Matrix Flow

While values of the calibrated parameters for the matrix flow regime are given in Table 1, water retention and hydraulic conductivity functions are shown in Fig. 3. The water retention curves for the macropore domain, with either n = 2 or n = 6, demonstrate a more immediate release of water with increased pressure head (Fig. 3). The 95% confidence intervals of optimized parameters are generally small compared with the inversely estimated values (Table 1). The saturated hydraulic conductivity, K_s, measured on the core sample taken from the laboratory soil column was approximately four times higher than the calibrated K_s, while the α parameter fit by RETC to the experimentally measured retention curve was approximately 2.4 times smaller than the optimized value.

A comparison between experimental and HYDRUS-simulated cumulative drain flow as a function of time demonstrates that the numerical model was able to capture both the water front arrival time and the cumulative drain flux (Fig. 4). The Nash–Sutcliffe (NS) efficiency was slightly greater than 0.99, suggesting a near-perfect fit between the simulated and observed values. The model also predicted reasonably well pressures heads measured in the laboratory using tensiometers (Fig. 5). Good agreement (i.e., NS = 0.97, 0.78, and 0.96 during infiltration and NS = 0.88, 0.84, and 0.89 during drainage for tensiometers at 10, 40, and 70 cm above the subsurface drain, respectively) between measured and predicted pressure heads 10, 40, and 70 cm above the subsurface drain demonstrates the ability of the numerical model to simulate well the subsurface drainage boundary condition (Fig. 5).

Surface-Connected Macropores

Flow conditions in the 55-cm-long, centered, surface-connected macropore were only slightly affected by the soil hydraulic parameters θ_r, θ_s, α, or n of the macropore domain. Flow conditions were affected mainly by the saturated hydraulic conductivity of the macropore; however, an increase in K_s of the macropore domain (i.e., from 4.0 to 60,000 cm h^{-1}), in an attempt to match the cumulative drain flux under these conditions, suggested an upper bound for K_s. Since there is a 20-cm-thick matrix layer between the bottom of the macropore and the drain (the top of the subsurface drain is 75 cm below the surface), an additional increase in K_s could not generate a further increase in cumulative drain flow. The cumulative drain flux remained constant when higher K_s values were used, as the entire macropore became almost instantaneously fully saturated. For example, K_s values of 100, 1000, 10,000, and 60,000 cm h^{-1} produced simulated cumulative drain flows of 7200, 10,200, 12,200, and 12,300 cm^3, respectively, compared with the observed cumulative drain flow of 15,200 cm^3. This cumulative drain flow was simulated only when a 70-cm-long, centered, surface-connected macropore was considered in the model.

Using the macropore K_s of 60,000 cm h^{-1}, the model was able to capture the more

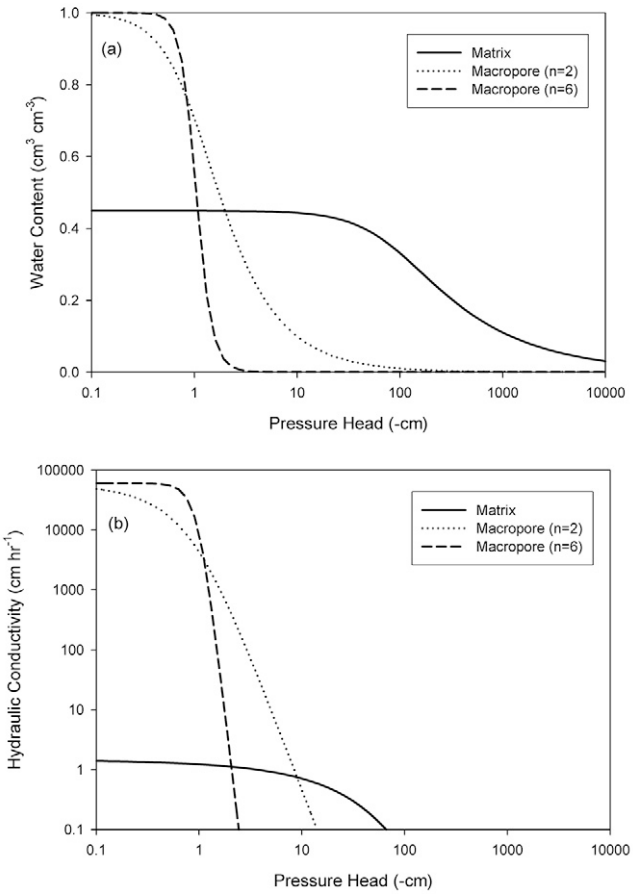

FIG. 3. Soil hydraulic functions representing the matrix and macropore domains: (a) soil moisture characteristic curve and (b) hydraulic conductivity function. Parameters for the matrix domain were obtained using inverse estimation. The n values for the macropore domain were selected as follows: n = 2 to represent a value for a typical soil and n = 6 to obtain an immediate release of water from saturated to residual moisture content.

TABLE 1. Soil hydraulic parameters† for the matrix and macropore domains using the van Genuchten (1980) model. The 95% confidence intervals are given for parameters optimized with either HYDRUS or RETC.

Domain	θ_r	θ_s	α	n	K_s	l	R^2
	— $m^3\ m^{-3}$ —		cm^{-1}		cm h^{-1}		
Core sample‡	0.03§	0.46 ± 0.01	0.005 ± 0.001	1.63 ± 0.24	6.22¶	–	1.0
Model, matrix#	0.03§	0.46§	0.012 ± 0.001	1.56 ± 0.08	1.46 ± 0.08	0.5	1.0
Model, macropore	0.00	0.46, 1.0††	0.1	2, 6††	60,000	0.5	–

† θ_r, residual volumetric water content; θ_s, saturated volumetric water content; α, n, and l, empirical parameters; K_s, saturated hydraulic conductivity.
‡ Fitted using RETC (van Genuchten et al., 1991).
§ Fixed (not fitted).
¶ Determined on undisturbed soil cores by the constant-head method.
# Estimated using HYDRUS (Šimůnek et al., 2006).
†† Used only for simulations with buried macropores.

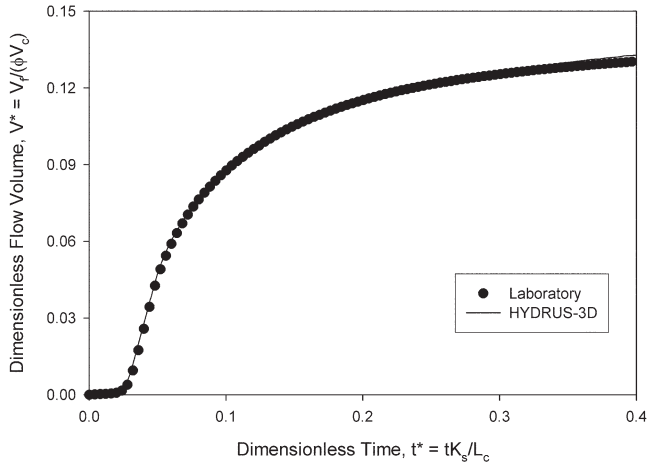

FIG. 4. A comparison of measured and model-calibrated dimensionless flow volume, V^* (where V_f = flow volume, ϕ = porosity, and V_c = column volume) vs. dimensionless time, t^* (where t = time, K_s = saturated hydraulic conductivity, and L_c = length of the column) for the column experiment without a macropore (i.e., matrix flow).

immediate response of laboratory tensiometers (Fig. 6) than when the flow system had no macropores (Fig. 5), although with lower NS values (i.e., NS = 0.41, 0.98, and 0.64, respectively, for the tensiometers 10, 40, and 70 cm above the drain) than the matrix flow simulation. The reason for the lower NS value for the tensiometer 10 cm above the drain was the lack of observed data due to the pressure exceeding the limit of the tensiometer. The model did not predict as rapid a response as observed at the tensiometer 70 cm above the drain (Fig. 5a). In general, the model performed better in matching the drainage part (i.e., 2–24 h) of the experiment (i.e., NS above 0.75 for all tensiometers) with the 55-cm, centered, surface-connected macropore than its infiltration part (i.e., 0–2 h). Figure 7 presents simulated pressure head profiles that show flow between the macropore and matrix on initiation of the infiltration due to hydraulic nonequilibrium conditions. This figure indicates the maximum pressure head of 55 cm observed at the bottom of the macropore. With increased time, the matrix wetting front progressed down the column and the pressure heads in the soil matrix surrounding the macropore increased due to lateral exchange between the macropore and matrix domains.

Simulations, as well as experimental data, showed a significant influence of the length of the centered, surface-connected

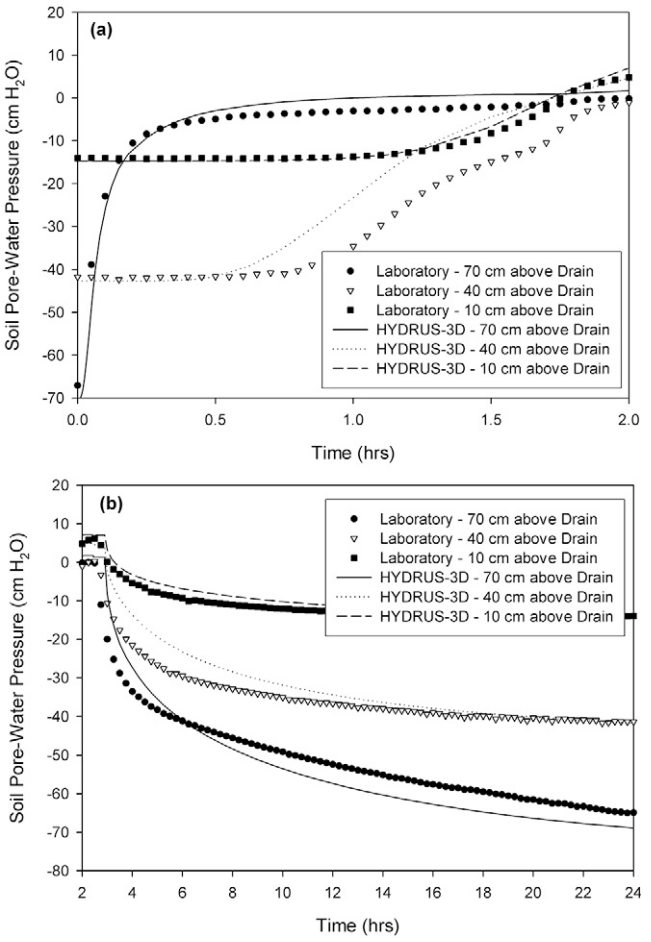

FIG. 5. A comparison of measured (averaged) and calculated pressure heads 70, 40, and 10 cm above the subsurface drain during the (a) infiltration and (b) drainage components of the column experiment without a macropore (i.e., matrix flow). The averaged values represent the mean of four tensiometers along a horizontal plane (12.5, 25.0, 31.5, and 38.0 cm from the left side) at the indicated height.

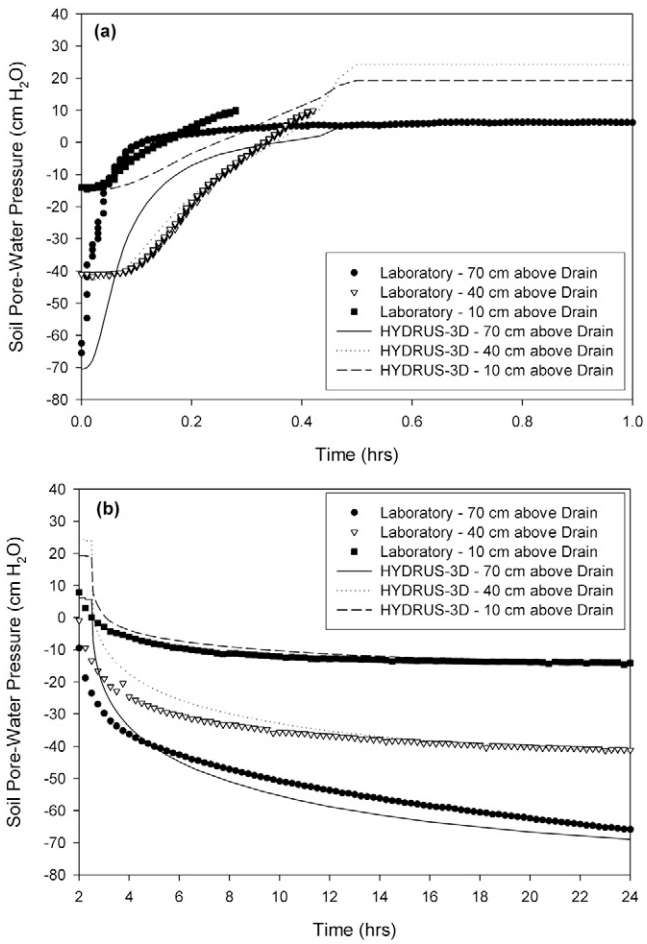

FIG. 6. A comparison of measured (averaged) and calculated pressure heads 70, 40, and 10 cm above the subsurface drain during the (a) infiltration and (b) drainage components on the soil column with the surface-connected, 55-cm-long macropore in the center of the profile. The averaged values represent the mean of four tensiometers along a horizontal plane (12.5, 25.0, 31.5, and 38.0 cm from the left side) at the indicated height.

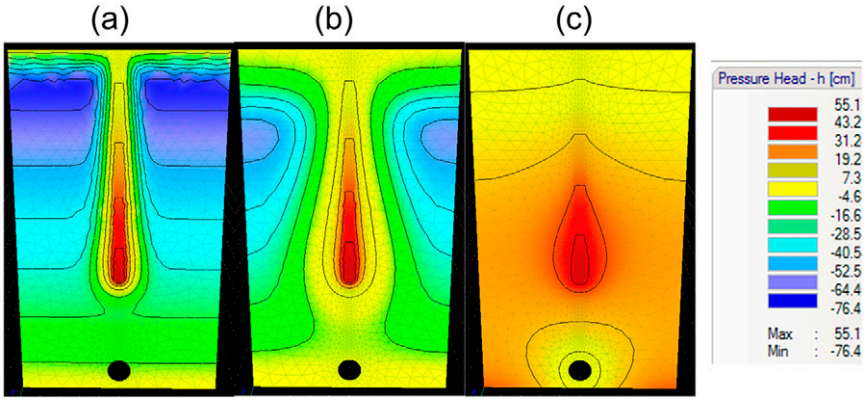

FIG. 7. Simulated pressure head profiles in the cross-section through the center of the soil column for the infiltration test with the surface-connected, 55-cm-long centered macropore at (a) 0.017 h, (b) 0.17 h, and (c) 0.5 h.

macropores on the drain flux. For example, 15-, 35-, 55-, and 70-cm-long macropores increased the drain flux approximately 1.03, 1.22, 1.60, and 2.41, respectively, compared with the case without macropores (Fig. 8). The effect of the macropore length on the drain flux, however, differs from the field observations of Shipitalo and Butt (1999), who observed no significant relationship between the burrow length and infiltration rates. While homogenous soil, as well as constant macropore characteristics, was achieved under the laboratory conditions, the field research of Shipitalo and Butt (1999) could not verify soil homogeneity and constant macropore properties in the field. Also, the field observations of Shipitalo and Butt (1999) were for soils that did not have subsurface drains. An open burrow length in the vicinity of the drain appears to be an important macropore characteristic for determining the potential effect on the drain flux and potentially could be even more important for contaminant transport. In fact, Allaire-Leung et al. (2000a,b) noted that the importance of macropore continuity seems to increase with an increase in the adsorption characteristics of the contaminant.

Under current domain dimensions and hydraulic conditions, the simulated arrival time for the soil column without macropores was 1.37 h, while it was 0.33 h for the soil column with the surface-connected, 55-cm-long, centered macropore that extended down approximately 75% of the distance to the drain. A sigmoidal relationship (R^2 = 0.998) was obtained between the length of surface-connected macropores and the simulated outflow arrival times when arrival times of all surface-connected macropores were considered (Fig. 9). This confirms that the bulk soil with a relatively slower water movement is largely bypassed when surface-connected macropores are introduced into the system.

The effect of surface-connected macropores on the increase of the steady-state discharge decreases with the lateral distance of the macropore from the drain, especially as the macropore penetration percentage increases. Total to matrix steady-state discharge became more uniform across all shifted distances when the macropore penetration of the shifted macropores decreased (Fig. 8). Since the 75-cm-long, centered, surface-connected macropore was directly connected also with the drain (i.e., pipe flow phenomena), the data point for this case is not included in Fig. 8. In this case, the cumulative drain flow becomes directly proportional to K_s.

The laboratory data for the soil profile with the 55-cm-long, surface-connected, centered macropore matched the results of

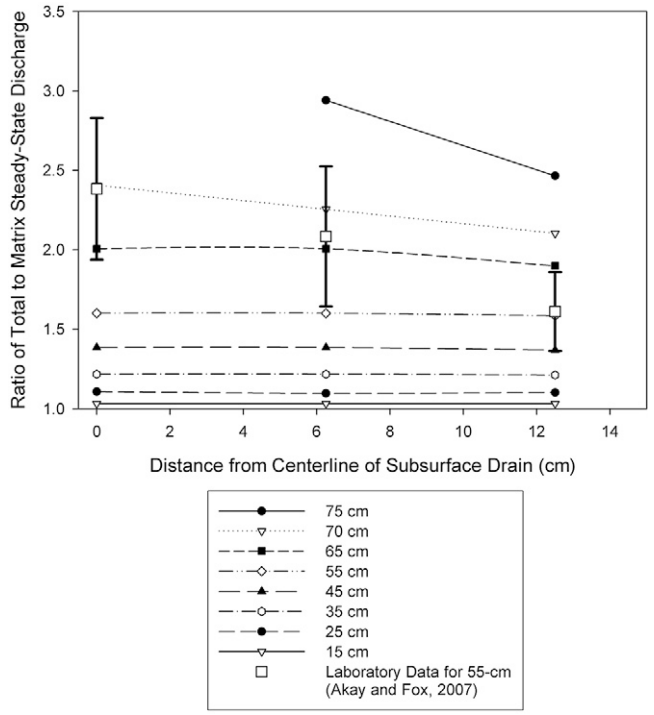

FIG. 8. Flux ratios vs. the lateral distance of the macropore from the drain. The flux ratio is the ratio between the steady-state flux for scenarios with macropores and the one without a macropore. Experimental data are for the soil column with the surface-connected, 55-cm-long macropore. Calculations were performed for macropores of different lengths. The flux ratio is 1 when there is no effect of the macropore on the steady-state flux. Error bars represent one standard deviation calculated from triplicate lab experiments. Lines represent HYDRUS simulation results.

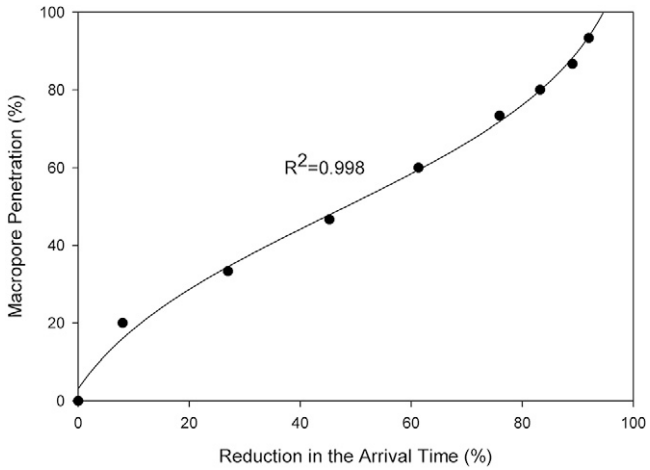

FIG. 9. Simulated reduction in the flow arrival time as a function of the macropore penetration for the soil column containing surface-connected macropores compared with conditions without macropores.

numerical simulations with the 70-cm-long, surface-connected, centered macropore; the 65-cm-long, surface-connected macropore shifted 6.25 cm away from the drain; and the 55-cm-long, surface-connected macropore shifted 12.5 cm away from the drain (Fig. 8). Several potential reasons exist for the discrepancies between the laboratory experiments and the numerical model. Because of the pressure heads generated, the most likely reason is fingering or additional preferential flow created in the laboratory experiments in the soil layer below the bottom of the macropore and the drain. This additional preferential flow had a larger impact on steady-state flux when the macropore was centered over the drain than when it was shifted away from the drain.

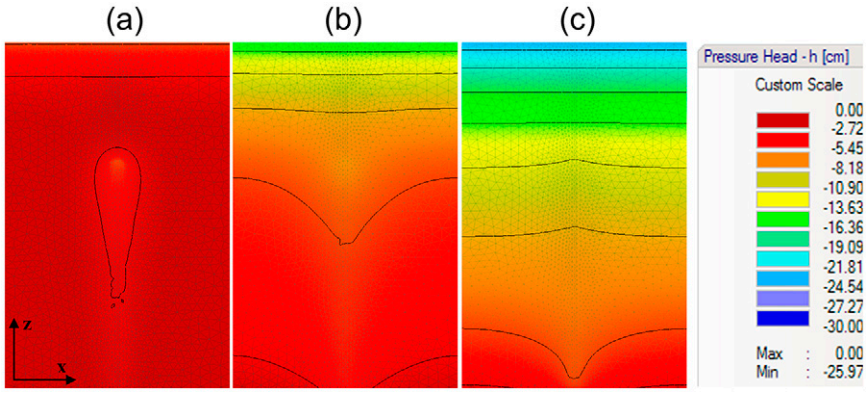

FIG. 10. Simulated pressure head profiles in the cross-section through the center of the soil column for the drainage test with the buried 55-cm-long centered macropore and the initial water table level at 80 cm at (a) 0.017 h, (b) 0.17 h, and (c) 0.5 h.

In general, the numerical simulations suggested an even greater contributing area with directly connected macropores than suggested by Akay and Fox (2007) and Fox et al. (2004). The need for calibration observed by Fox et al. (2007) is supported by these numerical simulations that show that the contributing area depends on the site-specific macropore depth of penetration.

Buried Macropores

Since buried macropores may be connected to the drain but not to the soil surface, the hydraulic conditions in the domain change drastically from conditions with surface-connected macropores (Fig. 10). The early hydraulic nonequilibrium observed during simulations with surface-connected macropores does not exist in simulations with buried macropores. The seepage face boundary condition could not be used for the section of the boundary where the buried macropore enters the subsurface drain since the model calculates here negative pressure heads, which leads to no-flux conditions. For this reason, the seepage face boundary condition was assigned around the drain, except for the buried macropore section. This part of the drain was assigned a zero pressure head boundary condition since this section was connected to the drain outlet. It should be noted that in tilled soils, buried macropores initiate at the interface between the plow layer and the soil matrix. These two layers may possess unique hydraulic properties. Therefore, a layered agricultural field soil with buried macropores could behave differently from the artificial soil system under study.

Simulations reflecting the practical conditions described above for controlled drainage practices, where the water table was initially above the subsurface drain, demonstrated that the percentage of macropore flow compared with the total drainage outflow (through both the matrix and macropore domains) ranged from 32 to 48% for $n = 2$ and from 19 to 43% for $n = 6$ (Table 2). For their imperfect drain condition where the water table built up over the drain, Akay and Fox (2007) observed that approximately 35% of the total flow came directly from 20- and 40-cm-long buried macropores and approximately 40% from 60- and 72-cm-long buried macropores. Distinctive responses of the matrix and buried macropore domains to drainage conditions are plotted in terms of cumulative outflow curves in Fig. 11. Although outflow from both domains started simultaneously, initially steep lines representing outflow from macropores

TABLE 2. The part of the drain outflow arriving directly through the buried macropore (n values of the van Genuchten [1980] model represent the macropore domain) for initial water table levels of +15, +35, +55, and +80 cm.

Buried macropore length	Drain outflow from buried macropore							
	+15 cm		+35 cm		+55 cm		+80 cm	
	$n = 2$	$n = 6$	$n = 2$	$n = 6$	$n = 2$	$n = 6$	$n = 2$	$n = 6$
	%							
15 cm	38.93	31.07	33.15	22.02	31.86	19.58	31.68	18.75
35 cm	39.70	31.64	41.38	33.62	39.06	29.47	38.55	28.29
55 cm	39.72	31.81	41.71	34.04	44.26	37.17	43.63	35.72
80 cm	39.81	31.97	41.80	34.24	44.51	37.61	48.30	42.91

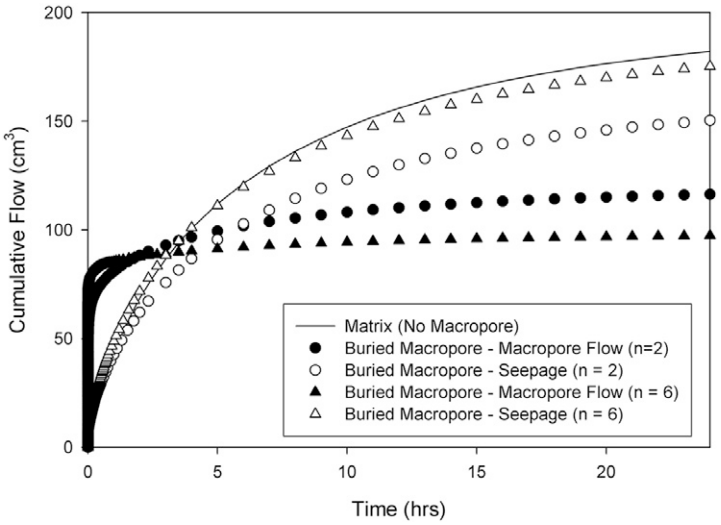

FIG. 11. Simulated cumulative macropore and matrix outflows for the drainage experiment with the buried 55-cm-long centered macropore. Initial water table was 80 cm above the drain. The n values for the macropore domain were selected as follows: $n = 2$ to represent a value for a typical soil and $n = 6$ to obtain an immediate release of water from saturated to residual moisture content.

suggested an immediate release of water from buried macropores. Even though this volume was higher than the matrix cumulative outflow during the first couple of hours, the overall contribution of the matrix reached about 60% of the total outflow in the long term. It should be noted here that these ratios could change depending on the hydraulic parameters and domain properties (i.e., a macropore radius and domain dimensions).

When water tables are initially above the subsurface drain, two variables are expected to significantly affect the water exchange between the matrix and macropore domains: the pressure gradient and the interfacial surface area between the macropore and matrix domains. The water table position determines the pressure gradient, whereas the length of the buried macropore determines the interfacial surface area. When the initial water table level is at or below the upper end of the buried macropore, the percentage of macropore flow is approximately the same and independent of the macropore length. The macropore flow contribution increases proportionally to the macropore length, however, when the initial water table is greater than the macropore length due to the increase in the interfacial surface area. For example, when the initial water level is 55 cm (n = 2), the percentage of macropore flow increases from 32 to 44% when the macropore length increases from 15 to 55 cm, and then remains approximately constant for longer (e.g., 80-cm) buried macropores (Table 2). For a given length of the buried macropore, the percentage of macropore flow maximizes when the water table is at an equivalent elevation to the macropore length. When the water table elevation further increases, the percentage of macropore flow decreases relative to the total matrix plus macropore flow. For example, for the buried 55-cm-long macropore (n = 2), the percentage of macropore flow increased from 40 to 44% when the initial water table was increased from 15 to 55 cm, respectively, and then decreased approximately 1% when the initial water table was at 80 cm (Table 2). This is due to the fact that the increase in macropore flow (5.8 cm^3) is smaller than the corresponding increase in matrix flow (11.1 cm^3), as shown in Table 3.

Summary and Conclusions

Several infiltration experiments previously conducted by Akay and Fox (2007) were simulated using HYDRUS. Model results demonstrated significant hydraulic nonequilibrium conditions between the matrix and macropore domains during infiltration into a soil column that contained surface-connected macropores. The hydraulic nonequilibrium was less pronounced for simulations involving buried macropores. In addition to previously used one- and two-dimensional dual-porosity and dual-permeability models to describe such conditions, the numerical solution of the three-dimensional Richards equation with two distinctive hydraulic functions for the matrix and macropore domains proved to be useful as well. Presented numerical simulations verified the model's ability to handle sharp interfaces between the two domains, with dramatically different soil hydraulic parameters. Simulations also confirmed the frequently observed relationships between drain flow and its arrival time with the macropore distance from the subsurface drain. The importance of the macropore's penetration distance on this relationship is highlighted. Reduction in flow arrival times for conditions with macropores compared with matrix flow conditions was directly related to the penetration depth. Numerical simulations suggested a greater contributing area (i.e., the region where the macropore has an effect on the total drain flow) with directly surface-connected macropores than suggested in the literature, with this area again depending on the macropore length. It should be researched further whether the contributing area should vary for water, tracers, and reactive contaminants. As the buried macropores could not be activated by surface infiltration of a limited duration, an alternative scenario with the water table initially above the subsurface drain was also simulated. Considering an immediate release of water from the drain-connected buried macropores and their further ability to transmit 30 to 40% of flow, the chemical composition of water in macropores can dictate the water quality in the outflow of the subsurface drains during early stages of drainage.

Acknowledgments

This project has been supported by the USDA Cooperative State Research, Education, and Extension Service (CSREES) NRI Seed Grant (2004-35102-14890) and USDA CSREES NRI Grant (2007-35102-18242).

References

Akay, O., and G.A. Fox. 2007. Experimental investigation of direct interconnectivity between macropores and subsurface drains during infiltration. Soil Sci. Soc. Am. J. 71:1600–1606.

Allaire-Leung, S.E., S.C. Gupta, and J.F. Moncrief. 2000a. Water and solute movement in soil as influenced by macropore characteristics: 1. Macropore continuity. J. Contam. Hydrol. 41:283–301.

Allaire-Leung, S.E., S.C. Gupta, and J.F. Moncrief. 2000b. Water and solute movement in soil as influenced by macropore characteristics: 2. Macropore tortuosity. J. Contam. Hydrol. 41:303–315.

Buttle, J.M., and D.G. Leigh. 1997. The influence of artificial macropores on water and solute transport in laboratory soil columns. J. Hydrol. 191:290–314.

Castiglione, P., B.P. Mohanty, P.J. Shouse, J. Šimůnek, M.Th. van Genuchten, and A. Santini. 2003. Lateral water diffusion in an artificial macroporous system: Modeling and experimental evidence. Vadose Zone J. 2:212–231.

Dorner, S.M., W.B. Anderson, R.M. Slawson, N. Kouwen, and P.M. Huck. 2006. Hydrologic modeling of pathogen fate and transport. Environ. Sci.

Table 3. Components of the total drain outflow coming from the matrix and the buried 55-cm-long macropore at the early (time t = 10 s) and final (t = 24 h) stage of drainage (n values of the van Genuchten [1980] model represent the macropore domain).

Initial water table level	Cumulative flow entering the drain								Total drainage amount			
	From the buried macropore				From the matrix							
	10 s		24 h		10 s		24 h		10 s		24 h	
	n = 2	n = 6	n = 2	n = 6	n = 2	n = 6	n = 2	n = 6	n = 2	n = 6	n = 2	n = 6
cm	cm^3											
+15	13.7	20.1	34.0	27.4	2.3	2.6	51.7	58.7	16.0	22.8	85.7	86.1
+35	27.7	43.6	75.6	62.2	4.4	5.5	105.7	120.5	32.1	49.1	181.4	182.7
+55	39.5	64.0	110.5	95.0	6.1	7.9	139.2	160.5	45.6	71.9	249.7	255.5
+80	39.4	64.0	116.3	97.3	6.1	7.9	150.3	175.2	45.5	71.9	266.6	272.5

Technol. 40:4746–4753.
Fox, G.A., R. Malone, G.J. Sabbagh, and K. Rojas. 2004. Interrelationship of macropores and subsurface drainage for conservative tracer and pesticide transport. J. Environ. Qual. 33:2281–2289.
Fox, G.A., G.J. Sabbagh, R.W. Malone, and K. Rojas. 2007. Modeling parent and metabolite fate and transport in subsurface drained fields with directly connected macropores. J. Am. Water Resour. Assoc. 43:1359–1372.
Geohring, L.D., P.E. Wright, T.S. Steenhuis, and M.F. Walter. 1999. Fecal coliforms in tile drainage effluent. ASAE Pap. 992203. Am. Soc. Agric. Eng., St. Joseph, MI.
Ghodrati, M., M. Chendorain, and Y.J. Chang. 1999. Characterization of macropore flow mechanisms in soil by means of a split macropore column. Soil Sci. Soc. Am. J. 63:1093–1101.
Hoorman, J.J., J.N. Rausch, T.M. Harrigan, W.G. Bickert, M.J. Shipitalo, M.J. Monnin, S.R. Reamer, F.E. Gibbs, M.I. Gangwar, H. Keener, and L.C. Brown. 2005. Research, educational, and technical assistance priorities for liquid manure application in the Midwest. Pap. 052062. *In* ASAE Annu. Int. Meet., Tampa, FL. 17–20 July 2005. Am. Soc. Agric. Eng., St. Joseph, MI.
Jamieson, R.C., R.J. Gordon, K.E. Sharples, G.W. Stratton, and A. Madani. 2002. Movement and persistence of fecal bacteria in agricultural soils and subsurface drainage water: A review. Can. Biosyst. Eng. 44: 1.1–1.9.
Joschko, M., H. Diestel, and O. Larink. 1989. Assessment of earthworm burrowing efficiency in compacted soil with a combination of morphological and soil physical measurements. Biol. Fertil. Soils 8:191–196.
Joy, D.M., H. Lee, C.M. Reaume, H.R. Whitely, and S. Zelin. 1998. Microbial contamination of subsurface tile drainage water from field applications of liquid manure. Can. Agric. Eng. 40:153–160.
Kladivko, E.J., J. Grochulska, R.F. Turco, G.E. Van Scoyoc, and J.D. Eigel. 1999. Pesticide and nitrate transport into subsurface tile drains of different spacings. J. Environ. Qual. 28:997–1004.
Köhne, J.M., and B.P. Mohanty. 2005. Water flow processes in a soil column with a cylindrical macropore: Experiment and hierarchical modeling. Water Resour. Res. 41:1–17.
Li, Y., and M. Ghodrati. 1997. Preferential transport of solute through soil columns containing constructed macropores. Soil Sci. Soc. Am. J. 61:1308–1317.
Magesan, G.N., R.E. White, and D.R. Scotter. 1995. Influence of flow rate on the concentration of indigenous and applied solutes in mole-pipe drain effluent. J. Hydrol. 172:23–30.
Phillips, R.E., V.L. Quisenberry, J.M. Zeleznik, and G.H. Dunn. 1989. Mechanism of water entry into simulated macropores. Soil Sci. Soc. Am. J. 53:1629–1635.
Shipitalo, M.J., and K.R. Butt. 1999. Occupancy and geometrical properties of *Lumbricus terrestris* L. burrows affecting infiltration. Pedobiologia 43:782–794.
Shipitalo, M.J., and W.M. Edwards. 1996. Effects of initial water content on macropore/matrix flow and transport of surface-applied chemicals. J. Environ. Qual. 25:662–670.
Shipitalo, M.J., W.M. Edwards, W.A. Dick, and L.B. Owens. 1990. Initial storm effects on macropore transport of surface-applied chemicals in no-till soil. Soil Sci. Soc. Am. J. 54:1530–1536.
Shipitalo, M.J., W.M. Edwards, and C.E. Redmond. 1994. Comparison of water movement and quality in earthworm burrows and pan lysimeters. J. Environ. Qual. 23:1345–1351.
Shipitalo, M.J., and F. Gibbs. 2000. Potential of earthworm burrows to transmit injected animal wastes to tile drains. Soil Sci. Soc. Am. J. 64:2103–2109.
Shipitalo, M.J., and F. Gibbs. 2005. Preferential flow of liquid manure in macropores and cracks. Pap. 052063. *In* Proc. Annu. Conf., Am. Soc. Agric. Biol. Eng., St. Joseph, MI.
Shipitalo, M.J., V. Nuutinen, and K.R. Butt. 2004. Interaction of earthworm burrows and cracks in a clayey, subsurface-drained soil. Appl. Soil Ecol. 26:209–217.
Šimůnek, J., N.J. Jarvis, M.Th. van Genuchten, and A. Gärdenäs. 2003. Review and comparison of models for describing non-equilibrium and preferential flow and transport in the vadose zone. J. Hydrol. 272:14–35.
Šimůnek, J., M.Th. van Genuchten, and M. Šejna. 2006. The HYDRUS software package for simulating two- and three-dimensional movement of water, heat, and multiple solutes in variably-saturated media. Tech. Manual. Version 1.0. PC Progress, Prague, Czech Republic.
Skaggs, R.W., M.A. Breve, and J.W. Gilliam. 1994. Hydrologic and water quality impacts of agricultural drainage. Crit. Rev. Environ. Sci. Technol. 24:1–32.
Skaggs, R.W., M.A. Breve, and J.W. Gilliam. 1995. Predicting effects of water table management on loss of nitrogen from poorly drained soils. Eur. J. Agron. 4:441–451.
Steenhuis, T.S., M. Bodnar, L.D. Geohring, S.A.E. Aburime, and R. Wallach. 1997. A simple model for predicting solute concentration in agricultural tile lines shortly after application. Hydrol. Earth Syst. Sci. 4:823–833.
Trojan, M.D., and D.R. Linden. 1992. Microrelief and rainfall effects on water and solute movement in earthworm burrows. Soil Sci. Soc. Am. J. 56:727–733.
van Genuchten, M.Th. 1980. A closed-form equation for predicting the hydraulic conductivity of unsaturated soils. Soil Sci. Soc. Am. J. 44:892–898.
van Genuchten, M.Th., F.J. Leij, and S.R. Yates. 1991. The RETC code for quantifying the hydraulic functions of unsaturated soils. Version 1.0. EPA Rep. 600/2-91/065. U.S. Salinity Lab., Riverside, CA.
Wesstrom, I., and I. Messing. 2007. Effects of controlled drainage on N and P losses and N dynamics in a loamy sand with spring crops. Agric. Water Manage. 87:229–240.